Indian Journal of Surgery
https://doi.org/10.1007/s12262-021-03228-9

ORIGINAL ARTICLE

Comparison of MRI Features of Invasive Pleomorphic and Classical Lobular Carcinoma: Differentiation Is Possible?

Temel Fatih Yilmaz[1] · Hafize Otcu[1] · Lutfullah Sari[1] · Zuhal Gucin[2] · Mehmet Ali Gultekin[1] · Fatma Celik Yabul[1] · Huseyin Toprak[1] · Seyma Yildiz[1]

Received: 11 January 2021 / Accepted: 10 December 2021

Abstract
To evaluate breast MRI and DWI and demographic features of pleomorphic invasive lobular carcinoma (pILC) and classic invasive lobular carcinoma (cILC). Invasive lobular (ILC) is the second most common breast malignancy after invasive ductal carcinoma (IDC) and constitutes the 8–14% of all invasive breast cancers. ILC morphologically can be classified into the classic, alveolar, solid, tubulolobular, and pleomorphic subtypes according to WHO. This study was performed retrospectively. The MRI and demographic features of 18 patients with 23 pILC were compared with those 22 consecutive patients with 27 cILC. There was no significant difference in demographic features of patients, MR appearance, kinetics, and ADC values between two groups. pILC, an aggressive subtype of ILC, cannot be differentiated from cILC with breast MRI.

Keywords Pleomorphic · Classical · Invasive lobular carcinoma · MRI · Breast cancer · WHO

Introduction

Invasive lobular (ILC) is the second most common breast malignancy after invasive ductal carcinoma (IDC) and constitutes the 8–14% of all invasive breast cancers [1]. ILC morphologically can be classified into the classic, alveolar, solid, tubulolobular, and pleomorphic subtypes according to WHO [1–3]

Pleomorphic invasive lobular carcinoma (pLIC), a special subtype of ILC, constitutes the approximately 15% of ILC (1). It has a more aggressive nature than classic invasive lobular carcinoma (cILC) [1, 4–8]. However, pLIC could not be differentiated from cILC based on classical imaging methods [4]. ILC may not form a palpable mass lesion and this accounts for the difficulty in its detection on physical examination [9, 11]. Routine imaging methods (mammography and ultrasound) are not very specific for ILC [9, 11]. Mammography (MG) and ultrasonography (US) play a limited role in ILC diagnosis and both modalities tend to underestimate lesion size [4, 5, 9, 11]. For this reason, Magnetic resonance imaging (MRI) is the proposed imaging modality for the evaluation of ILC.

To our knowledge, there has not been any report on the diffusion-weighted imaging (DWI) features of PILC compared to the classic ILC (cILC). The aim of this study was to evaluate breast MRI and DWI and demographic features of PILC and CILC and whether diffusion-weighted imaging (DWI) may play a role in differential diagnosis of both lesions.

Materials and Methods

The study was performed by retrospectively analyzing previous clinical, radiological, and pathological data from June 2013 to December 2019. It was approved by our institutional review board, and the informed consent requirement was waived due to retrospective design of the study. In this study, 18 patients with 23 pILC that were histopathologically confirmed were included. The MRI and demographic findings of these pILC patients were compared with those 22 consecutive patients with 27 cILC who were also diagnosed histopathologically.

✉ Lutfullah Sari
drlutfullahsari@gmail.com

[1] Department of Radiology, Faculty of Medicine, Bezmialem Vakif University, Istanbul, Turkey

[2] Department of Pathology, Faculty of Medicine, Bezmialem Vakif University, Istanbul, Turkey

Published online: 31 January 2022

MRI Protocol

All MR examinations were performed via a 1.5 Tesla MR (Magnetom Avanto, Siemens Healthcare, Erlangen, Germany) with a sixteen-channel CP Breast Array coil. Conventional sequences of routine breast MRI were performed for all patients by using axial fat-suppressed T2-weighted (TR/TE, 4560/59 ms; slice thickness, 4 mm; matrix, 340 × 512) sequences. One pre-contrast and five contrast-enhanced three-dimensional dynamic fat-suppressed axial T1-weighted fast low-angle shot sequences (TR/TE, 5.16/2.38 ms; flip angle, 10°; slice thickness, 1.1 mm; matrix, 320 × 512) were taken. Each of the five dynamic contrast-enhanced sequences took 60 s. Subtraction images were also obtained. 15 cc Gadobutrol (1.0 mmol/mL) was administrated, at a rate of 2 mL/s, with an automatic MR-compatible injector followed by 20-mL saline flush of the right antecubital vein.

The DW-MRI sequences were performed using three different b-value sets in the axial plane (b = 50, 400, 800 s/mm^2), with a two-dimensional echo-planar imaging (EPI) sequence (TR/TE, 8200/95 ms; flip angle, 90°; slice thickness, 3.5 mm; matrix, 192 × 192; signal average, 4) in the axial plane. Maximum-sized circular regions of interest (ROI) were placed within the primary lesions on the ADC maps by referring to DW-MRI or subtracted dynamic images. The ADC maps were created automatically by the system from the trace-weighted images with b values of 50 and 800. The following formula was used to calculate the ADC values: [ADC = 1/(b2-b1) × ln(S1/S2)] where the S1 and S2 values were the signal intensities at b values of [b1 = 50] and [b2 = 800] s/mm^2, respectively.

Analysis of MR Images

All the DCE-MR breast images and DW images were retrospectively and independently interpreted by one of two radiologists specializing in breast MR imaging without knowledge of pathologic findings. Any disagreement of interpretation was resolved by consensus. All MRIs were evaluated by the Workstation (Leonardo, Siemens Healthcare). Unenhanced, fat-suppressed images of the dynamic series were subtracted from the series of contrast-enhanced images in order to selectively differentiate the enhancing structures. In cases of multiple lesions in one breast, all the lesions were evaluated except the lesions with a diameter < 5 mm to optimize the ADC calculation. The largest diameter of the lesion was measured on a subtracted image from the series obtained 2 min after contrast injection. On dynamic MR images, ROI was placed at a lesion's most enhancing area for the purpose of obtaining time-signal intensity curves.

The 5th edition of American College of Radiology's Breast Imaging Reporting and Data System (BI-RADS®) [10] was the basis for describing the morphologic characteristics, enhancement patterns, and kinetic features of mass and distribution of non-mass enhancement (NME) [11]. Shapes of the lesions were oval or round or irregular. Margins were classified as circumscribed and irregular or spiculated. Internal enhancement characteristics had 3 options: homogeneous, heterogeneous, and peripheral. Two standpoints were used to evaluate the enhancement kinetics of the lesions. Initial signal increase is at the early contrast-enhanced phase of the peak percentage of the increase of signal intensity. This occurs during the wash-in rate, i.e., the first two contrast-enhanced acquisitions. A wash-in rate of more than 100% was defined as strong, between 50 and 100% as intermediate, and < 50% as slow enhancement. Second, post-initial signal behavior is the curve's shape after early phase enhancement (washout kinetics). Definitions of curves' types, based on delayed-phase enhancement all during the dynamiccourse, were persistent (signal intensity increase > 10%), plateau (signal intensity changed < 10%), and washout curves (> 10% reduction of the intensity of the signal).

The DWIs that formed the basis of our study were obtained prior to contrast-enhanced examination. Maximum-sized circular regions of interest (ROI) were placed within the primary lesions on the ADC maps by referring to DW-MRI and subtracted dynamic images. ADC values were obtained avoiding apparent necrotic or cystic components. The mean ADC values of voxels in the ROI were calculated for each lesion at least three times, the lowest reading of which was accepted as the value of the ADC. Mean ROI size was 50 mm^2 (range 25–700 mm^2). ADC values of lesions showing nonmass enhancement on DCE-MRI were not measured.

Statistical Analysis

Statistical analysis was performed using SPSS version 20.0 (SPSS Inc., New York, USA). The MRI and demographic features of pILC and cILC were compared using the chi-squared test (χ^2 test) or Fisher's exact test for categorical variables. The differences in lesions' size and ADC values between pILC and cILC were analyzed using *T*-test. A p value < 0.05 was considered statistically significant.

Results

In total, there were 18 patients with pILC and 22 patients with cILC. There was no significant difference in the mean age of patients in two groups (in PILC group mean age:

Table 1 Enhancement patterns of cILC and pILC

	pILC ($n=23$)	cILC ($n=27$)	p value
Non-mass enhancement ($n=3$, 6%)	2 (8.7%)	1 (3.7%)	0.58
Mass ($n=47$, 94%)	21 (913%)	26 (96.3) %	

54 ± 10.6 years; in cILC group mean age: 49 ± 11.7 years, p value: 0.145). Of 18 patients with pILC, three patients had two lesions in the same breast and one patient had three lesions in the same breast. Of 22 patients with cILC, four patients had two lesions in the same breast and one patient had one lesion (cILC) in one breast and two lesions in the other breast (tubular type ILC and cILC). Thus, in 40 patients, there were a total of 23 and 27 pathologically confirmed pILC and cILC lesions, respectively. Two pILC lesions and one cILC lesion showed segmentally distributed nonmass enhancement pattern on contrast-enhanced dynamic breast MRI. Remaining forty-seven lesions showed mass-like enhancement pattern (Table 1). There was no statistically significant difference in the appearance, kinetics, and ADC values between two groups (Tables 2 and 3) (Figs. 1 and 2).

Discussion

PLIC is a rare and distinct pathological variant of ILC with a poor prognosis; therefore, a few studies about imaging features of PLIC are present in the literature [4, 5, 12]. The radiologic features of pILC are not well-known, so radiologists are unfamiliar with pILC. Results of this study will help the clinicians in the differentiation of p ILC from cILC.

Tumor cells of ILC have distinctive loose infiltrative growth pattern and lack of desmoplastic stromal reaction. This results in difficulty of detection of ILC on MG which is used for both screening and detection (9,10). The sensitivity of MG for ILC ranges between 60 and 80% [9]. The most common mammographic manifestations of ILC are architectural distortion, spiculated or ill-defined masses with or without calcifications, and focal asymmetric densities [4, 5, 9]. Breast US is used primarily as a diagnostic tool to interrogate a suspicious mammographic abnormality. In literature, the overall sensitivity of US for the detection of ILC ranges between 68 and 98%, higher than mammography [9]. The most common sonographic findings of ILC are hypoechoic irregular or angular shaped solid mass with or without posterior acoustic shadowing and area of posterior acoustic shadowing without an associated mass [4, 9].

Table 2 DCE-MRI features and ADC values of pILC and cILC

		pILC (n = 21)	cILC(n = 26)	p value
Size		23 ± 23.03	27 ± 27.8	*0.272*
ADC		964.58 ± 206.32	907.90 ± 196.96	0.165
T2 signal	Hypointense	18	20	*n/a*
	Isointense	1	3	
	Hyperintense	2	3	
Margin	Circumscribed	0	1	0,15
	Irregular	5	12	
	Spiculated	16	13	
Shape	Oval	0	0	1,000
	Round	0	1	
	Irregular	21	25	
Contrast Enhancement	Homogeneous	2	2	*n/a*
	Heterogeneous	17	22	
	Rim enhancement	2	2	

Table 3 Signal intensity–time curve characteristics of pILC and cILC

Signal intensity/time curve		pILC ($n=21$)	cILC(n = 26)	p value
Initial enhancement	Medium	8, 38.1%	4, 15.4%	0.076
	Fast	13, 61.9%	22, 84.6%	
Delayed phase	Persistent (type 1)	0, 0%	2, 7.7%	0.335
	Plateau (type 2)	16, 76.2%	16, 61.5%	
	Washout (type 3)	5, 23.8%	8, 30.8%	

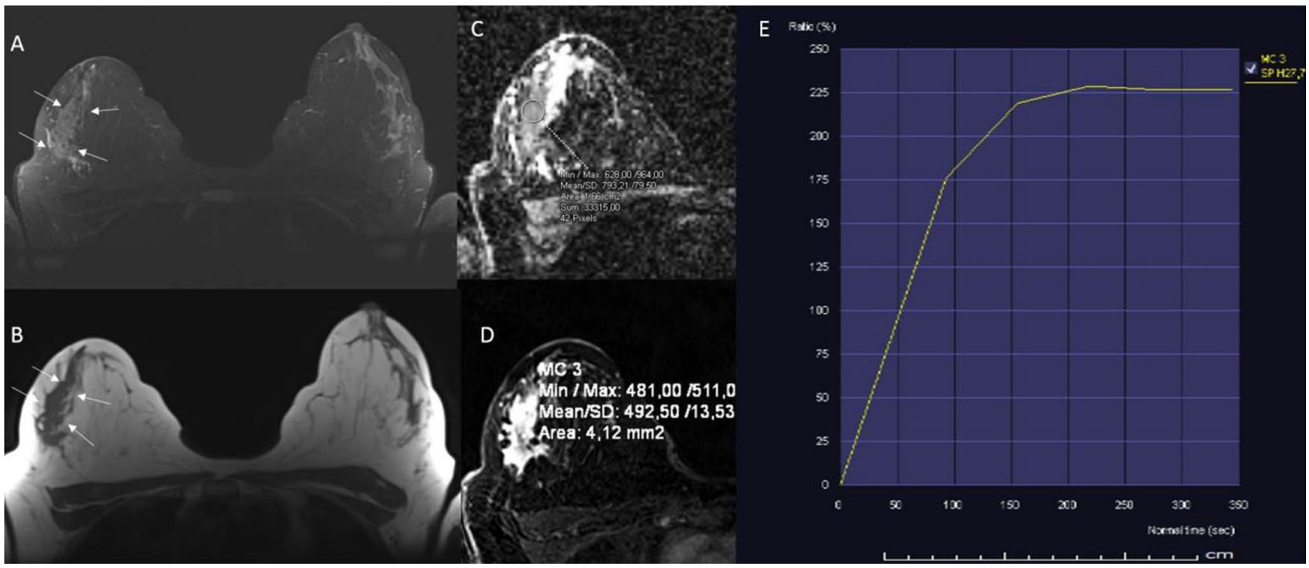

Fig. 1 **A**–**E** Axial fat saturated (**A**) and axial T1 weighted (**B**) images of right breast showed T2 hypointense and T1 hypointense irregular countered and shaped mass (arrows on **A** and **B**). On ADC map (**C**) that lesion restricts diffusion and measurement of ADC value (793×10^{-6}mm^2/s) by manually placed ROI was demonstrated. On subtracted contrast-enhanced T1 sequence (**D**), the lesion heterogeneously and strongly enhances. The signal intensity–time curve was type 2 (plateau). This lesion was pathologically confirmed pleomorphic invasive lobular carcinoma

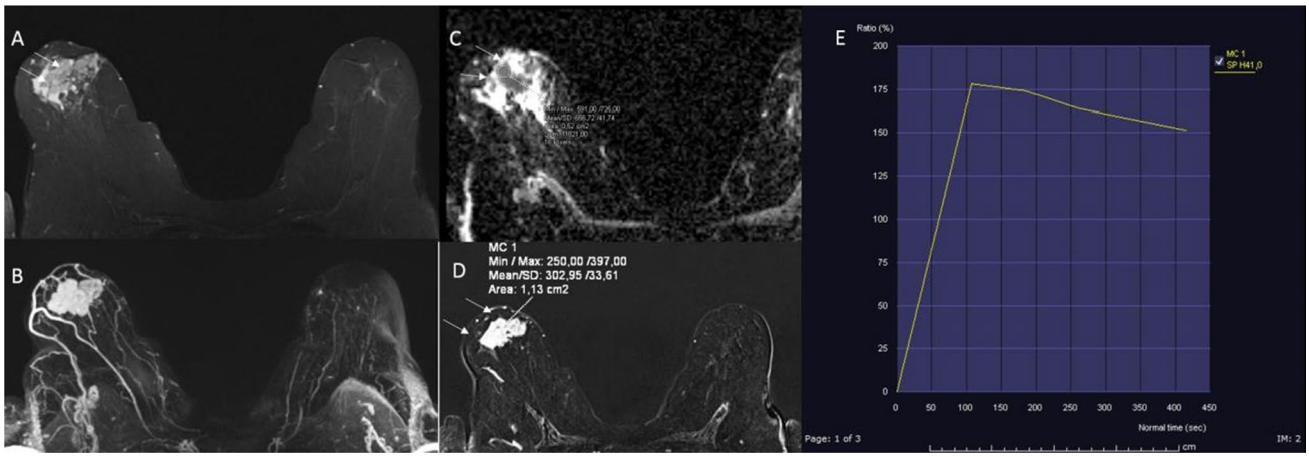

Fig. 2 **A**–**E** Axial fat saturated (**A**) and maximum intensity projection (MIP) (B) images of right breast showed T2 hypointense and T1 hypointense mass at retroareolar region (arrows on **A**). On ADC map (**C**), lesion shows restricted diffusion and measurement of ADC value (656×10^{-6}mm^2/s) by manually placed ROI was demonstrated. On subtracted contrast-enhanced T1 sequence (**D**), the lesion heterogeneously enhances (arrows on **D**). The signal intensity–time curve is type 3 (wash out). This lesion was pathologically confirmed as classic invasive lobular carcinoma

Due to relatively low sensitivity of US and especially MG in the diagnosis of ILC, dynamic contrast-enhanced breast MRI is nowadays widely accepted as the gold standard imaging modality for detection of ILC. Overall sensitivity of breast MRI for detecting ILC is 93% [9, 11]. With US and MG, cILC and pILC may be missed; therefore, in this study, we only evaluate MRI findings of pILC and cILC. In literature, there is only one study reporting MRI features of 13 pILC [4]. Our study is the second study and more comprehensive study compared to previous study of Jung.

Compared to cILC patients, pILC patients tend to be older and pILC mostly seen in postmenopausal period (2,13). In our study, the mean age of pILC was 54 years, slightly higher than cILC patients (mean age 49 years); but this is statistically not significant (p value: 0.145).

In this study, there was no statistically significant difference in the size, MR appearance, and kinetics between two groups. Similar to Jung et al., in our study, the size of pILC was slightly smaller than cILC (p value: 0,272) [4]. On MRI, morphology of ILC is often mass-like and a typical ILC seen as an irregular or spiculated mass with spiculated or ill-defined margins [9]. Sometimes non-mass like enhancement may be seen [4] Due to diffuse growth pattern of ILCs, areas of unexpected enhancement could also be seen. Asymmetrical enhancement pattern that can be ductal, segmental, regional, or diffuse may be the only sign of the tumor [9, 11]. Similar to previous studies, both pILC and cILC mostly presented as irregular-shaped lesions with spicular or irregular margins in our study. Data about the MR kinetics of cILC and pILC are limited. Jung et al. reported that both cILC and pILC showed washout about 70% [4]. Contrary to previous study of Jung, type 2 curve (plateau) was the most the common kinetic curve pattern in both pILC and cILC.

In our study, ADC values of pILC (mean $0.964 \times 10^{-3} mm^2/s$.) were slightly higher than values of cILC ($0.908 \times 10^{-3} mm^2/s$) but this is statistically insignificant. Breast cancers usually have a high cellularity and usually present with diffusion restriction and lower ADC values when compared to benign lesions [13–16]. Compared to cILC cells, pILC cells are larger than cILC cells and have abundant eosinophilic cytoplasm [4]. We thought that this histopathologic pattern of pILC results in slightly higher ADC values compared to cILC in spite of the fact that pILC has a more malignant nature. Routinely, combination of DCE-MRI with DWI increases the specificity without decreasing the sensitivity [12]. We suggested that in differentiation of cILC from pILC, DWI may not be useful as in other breast cancer subtypes.

For correct treatment of ILC, adequate staging is important. MRI demonstrates disease extent with a high reliability [11]. Previous studies showed that MRI is superior to conventional imaging (US and MG) in detection of ipsilateral and contralateral disease [9]. Detection of other lesions may improve surgical outcomes, decrease the recurrence rate, and improve overall disease free-survival. In our study, MRI revealed four ipsilateral pILC and four ipsilateral cILC and one contralateral cILC.

Our study has some limitations. First, it is a retrospective study. Second, the number of enrolled patients especially pILC was small due to the rarity of this variant.

Conclusion

pILC, an aggressive subtype of ILC, cannot be differentiated from cILC with breast MRI. Although these two subtypes of ILC could not be differentiated based on imaging findings, breast MRI should be performed in all patients with clinical suspicion of these tumors to plan appropriate treatment.

Data availability Not applicable.

Declarations

Ethics Approval All procedures performed in the studies involving human participants were in accordance with the ethical standards of the institutional and/or national research committee and with the 1964 Helsinki Declaration and its later amendments or comparable ethical standards.

Consent for Publication Not applicable.

Conflict of Interest The authors declare no competing interests.

References

1. Al-Baimani K, Bazzarelli A, Clemons M, Robertson SJ, Addison C, Arnaout A (2015) Invasive pleomorphic lobular carcinoma of the breast: pathologic, clinical, and therapeutic considerations. Clin Breast Cancer 15(421–25):2
2. Invasive lobular carcinoma (2019) Eds: Shin SJ, Desmedt C, Kristiansen G, Reis-Filho JS, Sasano H. in : WHO 5th edition: WHO Classification of Tumours. 5th edition. Breast Tumours, Lyon, pgs: 114–118.
3. Guiu S, Wolfer A, Jacot W, Fumoleau P, Romieu G, Bonnetain F, Fiche M (2014) Invasive lobular breast cancer and its variants: how special are they for systemic therapy decisions? Crit Rev Oncol Hematol 92:235–257
4. Jung HN, Shin JH, Han BK, Ko EY, Cho EY (2013) Are the imaging features of the pleomorphic variant of invasive lobular carcinoma different from classic ILC of the breast? Breast 22:324–329
5. Yeap PM, Evans A, Purdie CA, Jordan LB, Vinnicombe SJ (2018) A comparison of the imaging features of pleomorphic and classical invasive lobular carcinoma. Breast Cancer Res Treat 172:381–389
6. Iorfida M, Maiorano E, Orvieto E, Maisonneuve P, Bottiglieri L et al (2012) Invasive lobular breast cancer: subtypes and outcome. Breast Cancer Res Treat 133:713–723
7. Butler D, Rosa M (2013) Pleomorphic lobular carcinoma of the breast: a morphologically and clinically distinct variant of lobular carcinoma. Arch Pathol Lab Med 137:1688–1692
8. Haque W, Arms A, Verma V, Hatch S, Butler EB, Teh BS (2019) Outcomes of pleomorphic lobular carcinoma versus invasive lobular carcinoma. Breast 43:67–73
9. Johnson K, Sarma D, Hwang ES (2015) Lobular breast cancer series: imaging. Breast Cancer Res 17:94
10. Menezes GL, Knuttle FM, Stehouwer BL, Pijnapple RM, van den Bosch MA (2014) Magnetic resonance imaging in breast cancer: a literature review and future perspectives. World J Clin Oncol 5:61–70
11. Mann RM, Hoogeveeen YL, Blickman JG, Boetes C (2008) MRI compared to conventional diagnostic work-up in the detection and evaluation of invasive lobular carcinoma of the breast: a review of existing literature. Breast Cancer Res Treat 107:1–14
12. Kul S, Cansu A, Alhan E, Dinc H, Gunes G, Reis A (2011) Contribution of diffusion-weighted imaging to dynamic contrast-enhanced MRI in the characterization of breast tumors. AJR Am J Roentgenol 196(1):210–7

13. American College of Radiology (2013) ACR BI-RADs magnetic resonance imaging. In: ACR Breast Imaging Reporting and Data System, Breast Imaging Atlas. Reston, ACR
14. Gupta A, Sharma N, Jha AK, Gandgi A, Singh UR (2012) Pleomorphic variant of lobular carcinoma breast: a rare case report with review of the literature. J Cancer Res Ther 8:320–322
15. Jung SP, Lee SK, Kim S, Choi MY, Bae SY et al (2012) Invasive pleomorphic lobular carcinoma of the breast: clinicopathologic characteristics and prognosis compared with invasive ductal carcinoma. J Breast Cancer 15:313–19
16. Yildiz S, Toprak H, Ersoy YE, Malya FU, Bakan AA, Aralasmak A, Gucin Z (2018) Contribution of diffusion-weighted imaging to dynamic contrast-enhanced MRI in the characterization of papillary breast lesions. Breast J 24:176–179